Bioorganic & Medicinal Chemistry 22 (2014) 1804–1808

Contents lists available at ScienceDirect

Bioorganic & Medicinal Chemistry

journal homepage: www.elsevier.com/locate/bmc

Interaction kinetics of liposome-incorporated unsaturated fatty acids with fatty acid-binding protein 3 by surface plasmon resonance

Maria Carmen Tan [a,b], Shigeru Matsuoka [a,c,d], Hikaru Ano [a,d], Hanako Ishida [a], Mika Hirose [a,c], Fuminori Sato [a,d], Shigeru Sugiyama [a,c], Michio Murata [a,c,d,*]

[a] JST ERATO, Lipid Active Structure Project, Osaka University, 1-1 Machikaneyama, Toyonaka, Osaka 560-0043, Japan
[b] Department of Chemistry, De La Salle University, 2401 Taft Avenue, Malate, Manila 1004, Philippines
[c] Department of Chemistry, Graduate School of Science, Osaka University, 1-1 Machikaneyama, Toyonaka, Osaka 560-0043, Japan
[d] Project Research Center for Fundamental Science, Osaka University, 1-1 Machikaneyama, Toyonaka, Osaka 560-0043, Japan

ARTICLE INFO

Article history:
Received 13 December 2013
Revised 31 January 2014
Accepted 3 February 2014
Available online 13 February 2014

Keywords:
Fatty acid binding proteins
Large unilamellar vesicles
Surface plasmon resonance

ABSTRACT

The role of heart-type fatty acid-binding protein (FABP3) in human physiology as an intracellular carrier of fatty acids (FAs) has been well-documented. In this study, we aimed to develop an analytical method to study real-time interaction kinetics between FABP3 immobilized on the sensor surface and unsaturated C18 FAs using surface plasmon resonance (SPR). To establish the conditions for SPR experiments, we used an FABP3-selective inhibitor 4-(2-(1-(4-bromophenyl)-5-phenyl-1*H*-pyrazol-3-yl)-phenoxy)-butyric acid. The affinity index thus obtained was comparable to that reported previously, further supporting the usefulness of the SPR-based approach for evaluating interactions between FABPs and hydrophobic ligands. A pseudo-first-order affinity of FABP3 to K^+ petroselinate (C18:1 Δ6 *cis*), K^+ elaidate (C18:1 Δ9 *trans*), and K^+ oleate (C18:1 Δ9 *cis*) was characterized by the dissociation constant (K_d) near micromolar ranges, whereas K^+ linoleate (C18:2 Δ9,12 *cis*/*cis*) and K^+ α-linolenate (C18:3 Δ9,12,15 *cis*/*cis*/*cis*) showed a higher affinity to FABP3 with K_d around 1×10^{-6} M. Interactions between FAPB3 and C18 FAs incorporated in large unilamellar vesicles consisting of 1,2-dimyristoyl-*sn*-glycero-3-phosphocholine and FAs (5:1 molar ratio) were also analysed. Control DMPC liposomes without FA showed only marginal binding to FABP3 immobilized on a sensor chip while liposome-incorporated FA revealed significant responses in sensorgrams, demonstrating that the affinity of FAs to FABP3 could be evaluated by using the liposome-incorporated analytes. Significant affinity to FABP3 was observed for monounsaturated fatty acids (K_d in the range of 1×10^{-7} M). These experiments demonstrated that highly hydrophobic compounds in a liposome-incorporated form could be subjected to SPR experiments for kinetic analysis.

1. Introduction

The leading cause of human mortality is cardiovascular disease, which affects populations in both developed and developing countries, with an estimated predicted death rate of nearly 23.6 million by the year 2030.[1] Research in animal models has shown that fatty acid binding protein 3 (FABP3) maintains the energy homeostasis in the heart,[2] regulates lipid metabolism and adipose tissue development,[3] increases insulin sensitivity,[4] and controls dopamine D2 receptor function in the brain.[5] FABP3 levels in the serum have been shown to strongly correlate with body mass index but weakly with hypertension.[6] FABP3 presence in the blood has been identified as an early biochemical marker for acute myocardial infarction and Creutzfeldt–Jakob disease; FABP3 role as a possible tumor suppressor in breast adenocarcinoma has also been suggested.[6] In addition, it has been shown that FABP3 may interfere with the treatment of cardiovascular disease because certain specific drugs can act as FAPB3 inhibitors by interacting with the fatty acid binding site, which renders the drug inactive and causes

Abbreviations: CMC, critical micelle concentration; DMPC, 1,2-dimyristoyl-*sn*-glycero-3-phosphocholine; EDC, 1-ethyl-3-(3-dimethylaminopropyl)-carbodiimide; FABP3, fatty acid binding protein 3; FAs, fatty acids; k_a, association rate constant; k_d, dissociation constant; K_d, equilibrium dissociation constant; LUVs, large unilamellar vesicles; MLVs, multilamellar vesicles; MUFAs, mono-unsaturated FAs; NHS, N-hydroxysuccinimide; PI, 4-(2-(1-(4-bromophenyl)-5-phenyl-1*H*-pyrazol-3-yl)-phenoxy)-butyric acid; PUFAs, poly-unsaturated fatty acids; SPR, surface plasmon resonance.

* Corresponding author. Tel.: +81 6 6850 5774.
E-mail address: murata@chem.sci.osaka-u.ac.jp (M. Murata).

http://dx.doi.org/10.1016/j.bmc.2014.02.001
0968-0896/

dyslipidaemia. Very recently, Kumagai et al. has revealed the potential clinical use of Una-G belonging to the FABP family as a ligand-activated fluorescent probe for detecting a biomarker.[7]

Fatty acids (FAs) in the cell cytosol originate from dietary lipids and de novo lipogenesis from carbohydrates. FA metabolism by β-oxidation in peroxisomes and mitochondria and ω-oxidation in microsomes require carrier proteins. Cytosolic carriers are also necessary for FAs to act as effectors of nuclear transcription and to be stored in adipocytes as triacylglycerides. FABPs represent a family of abundantly produced intracellular proteins involved in the transport of FAs. FABPs are relatively small 15-kDa polypeptides containing an N-terminal helix-turn-helix motif (αI–αII) that caps one end of the β-barrel formed by 10 anti-parallel strands.[8] Among 12 FABP isoforms, FABP3 constitutes 4–8% of the total cytosolic proteins in the mammalian heart and is ubiquitously expressed in both cardiac and skeletal muscle and marginally in the stomach, brain, lungs, and mammary glands.[9,10] The helical N-terminus was shown to participate in the regulation of FA transfer to intracellular membranes through collision transfer interactions.[11,12] This 'portal hypothesis' states that an FA molecule enters solvent-accessible area of FABP through a dynamic region comprising the α-helix II and βC–βD and βE–βF turns before binding to the pocket.[13] Non-specific interactions with FABP3 hydrophilic surface as well as conformational changes facilitate FA binding and subsequent entering into the hydrophobic cavity of FABP3[14,15] while the carboxylate group as shown by X-ray crystallography is buried in the core of the protein.[16]

Surface plasmon resonance (SPR) is considered one of the most powerful techniques for evaluating the affinity kinetics of molecular interactions in biological systems. Kinetic analysis enables label-free, real-time investigation of biomolecular hydrophobic interactions; SPR-based biosensors allow accurate estimation of distinct association/dissociation rate constants and equilibrium status parameters in different reaction models. In order to mimic biochemical/biomedical conditions, SPR analysis has to be carried out in aqueous media and is therefore largely applied to binding studies of water-soluble ligands immobilized on a sensor chip. Recently, considerable progress has been made toward structure elucidation of membrane-associated receptors and lipid bilayers by casting membranes on the sensing surface.[17] On the other hand, highly hydrophobic biomolecules such as lipids and sterols, which often play an essential role in signal transductions and other physiological events, are still troublesome analytes because of their poor water solubility. In the present study, we have established the experimental conditions for evaluating interactions between FABP3 and a hydrophobic inhibitor by SPR, and attempted to estimate the binding affinity between FABP3 and long-chained FAs incorporated into large unilamellar vesicles (LUVs).

2. Materials and methods

2.1. Material

4-(2-(1-(4-Bromophenyl)-5-phenyl-1*H*-pyrazol-3-yl)-phenoxy)-butyric acid, a protein inhibitor (PI) for FABP3, was synthesized according to the previously reported method.[18] Free petroselinic, elaidic, oleic, linoleic, and α-linolenic acid were purchased from Sigma–Aldrich (St. Louis, MO), and treated with 1 M potassium hydroxide in methanol to be converted into potassium (K^+) salts. N-hydroxysuccinimide (NHS), ethanolamine, 1-Ethyl-3-(3-dimethylaminopropyl)-carbodiimide (EDC), 10 mM sodium acetate buffer (pH 4.5), 50 mM sodium hydroxide (NaOH), 0.5% (w/v) sodium dodecyl sulfate (SDS), and 10× PBS running buffer (detergent free, pH 7.4) were obtained from GE Healthcare (Uppsala, Sweden). Dimethyl sulfoxide (DMSO) was purchased from Sigma–Aldrich. All other chemicals were of analytical grade.

2.2. Purification and delipidation of FABP3

The human *FABP3* gene (hFABP3) was synthesized with an N-terminal *Nde*1 site and C-terminal *Bam*H1 site. The 399-bp fragment was ligated into the *Nde*1/*Bam*H1-digested pET21a vector (Novagen, Madison, WI) and the expression plasmid pET21a hFABP3 was used to transform *Escherichia coli* BL21 (DE3). The expression of hFABP3 was induced by adding isopropyl-β-D-thiogalactopyranoside to the culture medium. Bacteria were grown as previously described,[19] harvested by centrifugation, sonicated, and centrifuged at 100,000*g* for 30 min at 4 °C. The supernatant was fractionated with ammonium sulphate and the appropriate fraction was dialyzed against 50 mM Tris–HCl (pH 8.0). The dialysate was passed through an anion exchange Hitrap DEAE FF column equilibrated with 50 mM Tris–HCl (pH 8.0), concentrated by ultrafiltration, and purified by size-exclusion column chromatography; refolding after delipidation was then performed.

2.3. Liposome preparation

LUVs were prepared by thin film hydration, freeze-thaw and subsequent extrusion. Lipid thin films were formed by dissolving 30 mg of 1,2-dimyristoyl-*sn*-glycero-3-phosphocholine (DMPC) without or with FA K^+ salts (5:1 molar ratio) in 6 mL $CHCl_3$ in a round bottom flask. The resultant solution was mixed thoroughly, evaporated, and the obtained film was further dried under vacuum for 12 h. The lipid film was then hydrated and suspended in 1 mL of running buffer (PBS, pH 7.4, with or without 5% DMSO). The suspension was sonicated and subjected to 5 cycles of freezing (−80 °C), thawing (60 °C), and vortexing (5 s) to form multilamellar vesicles (MLVs). The MLV suspension was passed through a double 0.1-μm-polycarbonate membrane filter 19 times with LiposoFast-Basic extruder (Avestin Inc., Ottawa, Canada) to form LUVs. The FA and DMPC concentrations of the solution were determined by the Free Fatty Acid Quantification Colorimetric/Fluorometric Kit (BioVision, Inc., Milpitas, CA) and Phospholipid *C*-Test (Wako Pure Chemical Industries Ltd, Japan) respectively, and the liposomes were diluted with PBS (pH 7.4) to give final FA concentrations of 20, 40, 60, and 80 μM.

2.4. Interaction measurements by SPR

The SPR biosensing investigations were performed at a controlled temperature of 25 °C using an FABP3-modified carboxylated dextran matrix (CM5) chip and analysed using the BIAcore T200 system (GE Healthcare). The unmodified CM5 sensor chip was washed 3 times with 50 mM NaOH at a flow rate of 20 μL/min for 2 min. Pre-concentration tests using 10 mM sodium acetate buffer at pH 4.0, 4.5, 5.0, and 5.5 showed the optimum binding at pH 4.5. FABP3 was covalently immobilized on the CM5 sensor chip using a modified amine coupling technique on a flow cell 2 or 4; cells 1 and 3 were unaltered and used as a reference. Surface activation was induced by injecting 70 μL of 0.1 M NHS mixed with 0.39 M EDC (1:1, v/v), at a flow rate of 5 μL/min for 7 min. FABP3 (100 μg/mL) was passed at 2 μL/min for 30 min over the sensor chip surface. NHS ester groups were deactivated with 1 M ethanolamine hydrochloride (pH 8.5) and the resulting surface was washed 3 times with running buffer (PBS pH 7.4 with or without 5% DMSO) to remove unbound species. The acceptable immobilization levels (referred to as bound and final FABP3 responses) were between 9000 and 13,000 response units (RU). Mass transfer limitation analysis did not show any significant variations in the rate constants depending on flow rates (5, 15, or 75 μL/min); therefore, all experiments were performed at a flow rate of 10 μL/min. Dissociation time (complete elution of the sample) was either 50 or 120 s. In each kinetic analysis, a blank run with only running buffer

was performed to control for any background interferences. The surface was regenerated by 0.5, 5, 10 mM NaOH or 10 mM glycine, pH 3.0. Regeneration parameters were based on the strength of interactions between the analyte and ligand. Data analysis incorporated double negative control reference from the blank run and parallel flow cell with unmodified surface to subtract bulk refractive index from the binding response. Resulting sensorgrams were analysed using the BIAcore T200 Evaluation Software Version 1.0.

Petroselinic, elaidic, oleic, linoleic, and α-linolenic acid K^+ salts were analysed by the affinity to FABP3; binding experiments were performed in triplicate. K^+ elaidate, oleate, and linoleate were dissolved in detergent-free PBS (pH 7.4) with 5% DMSO, and petroselinate and linoleate were diluted in PBS (pH 7.4) to the concentrations from 20 to 80 μM. Kinetic analyses for the monounsaturated FA (MUFA) K^+ salts were performed using association and dissociation times of 50 s each; elution of the bound material and regeneration of the sensor surface were performed by 0.5 mM NaOH at a flow rate of 10 μL/min for 50 s. K^+ linoleate and α-linolenate demonstrated the optimum binding at association and dissociation times of 120 s each, and the bound species were removed by 0.5 mM NaOH at a flow rate of 10 μL/min for 120 s. LUVs (20 to 80 μM of FA concentration prepared from DMPC or DMPC with FAs were passed over the immobilized FABP3 in PBS, pH 7.4, at a flow rate of 10 μL/min with an injection time of 120 s and dissociation of 300 s. The regeneration by 20 mM NaOH was performed for 120 s at a flow rate of 10 μL/min. PI at concentrations of 2, 4, 8, 12, 16 μM in 5% DMSO-containing PBS was passed over the sensor surface for 120 s, as an optimum analyte association time. Association and dissociation time was programmed for 120 s at a flow rate of 10 μl/min for each step according to the protocol of Beniyama et al.[17] Regeneration or removal of bound material was done by 5 mM NaOH at 10 μL/min for 300 s.

2.5. Data analysis

Analytes with clear binding to the immobilized FAPB3 detected by sensorgrams were processed using a 1:1 interaction (Langmuir interaction), heterogeneous ligand model, and a two-state reaction model. Best fits of the kinetic interaction models were dictated by the congruency of the simulated sensorgram superimposed on the sample sensorgram by curve fitting with BIAcore T200 Evaluation version 1.0. Global fitting, that is simultaneous fitting of the sensorgrams representing different concentrations of the same analyte, was performed for all trials but was not compatible with all analysed compounds, and evaluation through local fitting of sensorgrams was performed in these cases. Concentration-dependent aggregate formation in the aqueous phase could have led to the inconsistencies found in the kinetic parameters.[20] Langmuir interaction (a pseudo-first order reaction) was observed in some sensorgrams since interaction was dependent on one analyte. The details of data analysis are provided in Supporting information.

3. Results and discussion

We first examined 4-(2-(1-(4-Bromophenyl)-5-phenyl-1*H*-pyrazol-3-yl)-phenoxy)-butyric acid (PI) shown to be an FABP3-selective inhibitor[17] and the lead compound of this series of inhibitors originally described by Silsky et al. in Bristol Myers–Squibb.[21] FABP–PI interactions have been investigated based on SPR analysis by the same authors,[18] although the experimental details have not been published. Thus, we regarded PI as an ideal compound for testing our SPR protocol with the recombinant apo-FABP3. Consistent with the previous report,[18] PI was found to bind FABP3 with

Table 1
Kinetic parameters of PI for binding to FABP3 from the 1:1 interaction model

	Present values[a]	Reported values[17]
k_a ($\times 10^2$ M^{-1} s^{-1})	77.6 ± 8.4	58.3
k_d ($\times 10^{-2}$ s^{-1})	1.64 ± 0.47	1.92
K_d ($\times 10^{-6}$)	2.11 ± 0.40	3.30
R_{max} (RU)	62.5 ± 0.73	
Chi^2(RU^2) ($\times 10^1$)	1.00 ± 0.34	

[a] These values were obtained at 16 μM of PI while the global fitting protocol for the concentration of PI from 2 to 16 μM gave rise to a similar K_d value, 3.86×10^{-6}.

the equilibrium dissociation constant K_d of 2.11 μM (Table 1, Fig. S1 for sensorgrams). The best fit with the theoretical curve was obtained with the 1:1 interaction model; a similar K_d value of 3.86 μM was determined based on the global fitting. These results clearly demonstrate that these SPR conditions could be applied to studying kinetic interactions between FABP3 and hydrophobic analytes (Figure 1).

Using the established experimental conditions, we next examined the kinetics of FAs binding to FABP3. Among the biologically important FAs, we mostly focused on MUFAs because saturated or poly-unsaturated FAs (PUFAs) behaved differently and required further optimization of the conditions. K^+ petroselinate, elaidate, and oleate in concentrations from 20 to 80 μM, which were far below the critical micelle concentration (CMC), were passed over the chip-immobilized FABP3. A pseudo-first order kinetics or Langmuir binding model had the best correlation for all the tested MUFAs with K_d values from 1×10^{-5} to 1×10^{-4} M (Table 2); Figure 2 depicts the sensorgram for K^+ oleate while Figure S2 for K^+ petroselinate and K^+ elaidate. Among them, petroselinate displayed the highest affinity followed by oleate and elaidate. Global fitting analyses were not compatible to individual or locally fitted modes, especially in regard to the association rate constant k_a, since the molecular aggregate states of amphiphilic compounds are known to greatly depend on FA concentrations, which should influence the binding step.[22]

In the next step, LUVs were analysed by SPR to test whether they could be used as analyte carriers. LUVs used in the analysis consisted of DMPC approximately 100 nm in diameter (Table 3). DMPC concentrations in the resulting LUVs determined by the Phospholipids C colorimetric assay were from 0.285 to 0.300 M. As shown in the sensorgram (Fig. S3) of DMPC liposomes without fatty acid, the k_a values (Tables 3 and S1) appeared to be very low, indicating that binding of DMPC liposomes to the sensor chip was very weak. However, once DMPC was bound to the chip surface, dissociation was found to be very slow and dissociation

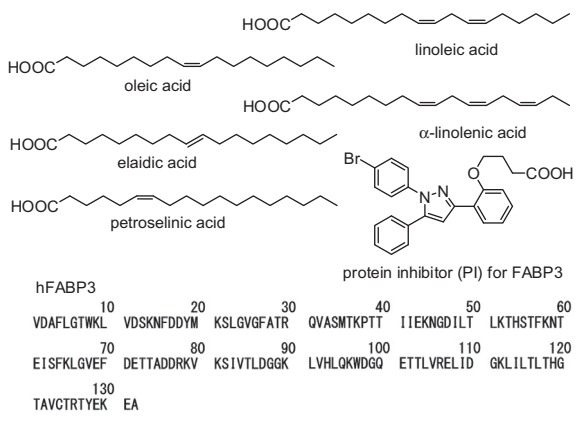

Figure 1. Structures of compounds and sequence of hFABP3 used in SPR experiments.

Table 2
Kinetic parameters for MUFAs as K^+ salts (60 μM) from a 1:1 interaction model

	K^+ petroselinate	K^+ elaidate	K^+ oleate
k_a ($\times 10^2$ M^{-1} s^{-1})	4.50 ± 0.20	0.37 ± 0.11	5.16 ± 0.69
k_d ($\times 10^{-2}$ s^{-1})	2.44 ± 0.01	1.33 ± 0.33	3.78 ± 0.09
K_d ($\times 10^{-6}$)	54.2 ± 0.23	359 ± 117	73.3 ± 0.90
R_{max} (RU)	1640 ± 70	165 ± 55	1510± 380
Chi^2 (RU^2) ($\times 10^1$)	3.36 ± 0.91	1.19 ± 0.16	7.04 ± 0.81

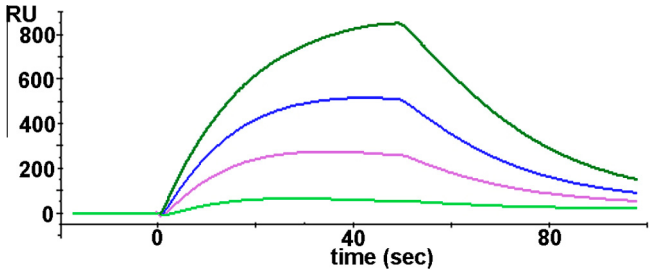

Figure 2. SPR sensorgrams for binding between FABP3 (ligand) and oleic acid K^+ salts (analyte). Background subtracted sensorgrams from 20 (bottom), 40, 60 and 80 (top) μM of K^+ oleate.

Table 3
Kinetic parameters for DMPC liposomes (60 μM) locally fitted from a 1:1 interaction model

k_a ($\times 10^2$ M^{-1} s^{-1})	0.34 ± 0.05
k_d ($\times 10^{-2}$ s^{-1})	ca. 0.00001
K_d ($\times 10^{-6}$)	0.0036 ± 0.0003
R_{max} (RU)	78.1 ± 4.1
Chi^2 (RU^2)($\times 10^{-1}$)	4.65 ± 0.37 × 10^{-1}

constant k_d was in the range of 1×10^{-9} M for both locally and globally fitted sensorgrams, which indicated strong interaction at the binding site. These findings revealed that DMPC in small amounts (less than 10 RU) bound to and stayed on the sensor chip surface during the experimental period, while a negligible amount of DMPC detached from the chip. When compared by k_a, the values for the tested MUFAs (see Table 4) were more than 20 times higher than this for DMPC, thus allowing us to estimate FA binding kinetics by directly fitting the data to theoretical models.

We prepared MUFA-containing LUVs (100 nm diameter) by using FA to DMPC molar ratio of 1:5. To examine FA influence on the liposome size, LUVs were subjected to dynamic light scattering analysis (Fig. S4), which revealed that the addition of MUFAs resulted in insignificant reduction of liposome sizes; LUVs containing 16.6 mol % MUFAs had an expected diameter of 100 nm. The SPR experiments using MUFA-incorporating liposomes showed interactions typical for ligand-analyte binding with K_d values in the submicromolar range; Figure 3 depicts the sensorgram for oleate in liposomes while Figure S5 for petroselinate and elaidate in liposomes. A prolonged interaction of the MUFA-containing liposomes and FABP3 was observed owing to higher affinity. Global fitting produced the results (Tables S3–S5) consistent with the locally fitted k_a, k_d and K_d.

Table 4
Kinetic parameters for 10 μM MUFAs in DMPC liposomes (total lipid concentration of 60 μM) based on locally fitted with the 1:1 interaction model

	K^+ petroselinate	K^+ elaidate	K^+ oleate
k_a ($\times 10^2$ M^{-1} s^{-1})	17.2 ± 0.48	37.7 ± 2.70	6.90 ± 1.02
k_d ($\times 10^{-2}$ s^{-1})	0.069 ± 0.009	0.028 ± 0.0003	0.011 ± 0.0006
K_d ($\times 10^{-6}$, M)	0.401 ± 0.0042	0.074 ± 0.0046	0.159 ± 0.0082
R_{max} (RU)	55.6 ± 3.9	186 ± 0.8	304.3 ± 2.8
Chi^2(RU^2) ($\times 10^{-1}$)	6.99 ± 0.81	2.00 ± 0.04	1.92 ± 0.14

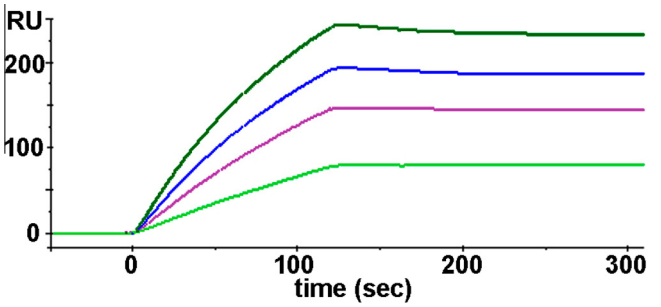

Figure 3. SPR sensorgrams for binding between FABP3 (ligand) and oleic acid K^+ salt in DMPC liposomes (analyte). Background subtracted sensorgrams from 20 (bottom), 40, 60 and 80 (top) μM of K^+ oleate incorporated in liposomes at the oleate-DMPC molar ratio of 1:5.

According to the affinity parameters between FAPB3 and FAs measured by radio-ligand binding experiments,[23] the K_d value for oleate was estimated to be 0.43 μM, which was somewhat weaker than the values in Table 4. A slightly lower K_d value observed in the present SPR study may partly be accounted for by the lower dissociation rate k_d because the residual DMPC bound on the sensor tip surface slows down the dissociation of FA. By comparing the kinetic parameters presented in Tables 2 and 4, it can be concluded that the liposome-based approach (Table 4) provides a more reliable way to evaluate FAs interactions with FABP3. The R_{max} values of petroselinate and oleate in Table 2 exceed the theoretical amount of the maximum binding of FA (200–300 RU), thus implying that non-specific binding constituted a larger part of their SPR responses; relative lower R_{max} of elaidate may be due to its higher melting point than other *cis*-MUFAs,[24] which decreases solubility and effective concentration of monomeric elaidate in the running buffer.[25] Higher k_d values in Table 2 may also be attributed to a lower affinity in non-specific binding.

A representative of PUFAs, K^+ linoleate (C18:2 Δ 9,12) was subjected to SPR analysis in solution at concentrations below CMC and in the liposome-embedded form. In solution, K^+ linoleate demonstrated a K_d in the micromolar range comparable to those of MUPAs (Table S5). On the other hand, the liposome preparations showed much higher affinity, but an accurate estimation of K_d value could not be performed because of extremely slow dissociation rate. As another example of PUFAs, K^+ α-linolenate (C18:3 Δ 9, 12, 15) kinetic interactions were examined and it revealed short-lived (15 s) non-specific binding to the sensor surface (data not shown). However, incorporated in the liposomes, K^+ α-linolenate demonstrated higher affinity (Table S6) as was the case with linoleate. The reason for the observed slow dissociation from the sensor chip surface is currently unknown.

Among saturated FAs, we examined short-chained K^+ decanoate and undecanoate because they can be easily dissolved in water whereas longer-chained saturated FAs with higher Krafft points such as stearic acid have limited solubility and difficulty in emulsifying in buffer. Nevertheless, no significant response (less than 3.0 RU) was observed in the sensorgrams upon addition of decanoate or undecanoate at the concentration of 120 μM without liposomes (data not shown).

The present study demonstrated the utility of liposomes as carriers of lipid compounds in binding studies based on SPR. The proposed method, however, provided unsatisfactory results for PUFAs largely because of their low dissociation from the chip surface. Other limitations of the method include lipid accumulation on the surface of the tubing and other connections along the flow routes, and this sometimes hampers the reproducibility of the binding kinetics. More frequent washing and renewal of the tubing system was necessary in the current experiments.

4. Conclusion

We evaluated the affinity between FA salts and FABP3 by SPR. While the usual aqueous preparation of FAs resulted in non-specific interactions or lack of binding, MUFAs incorporated in DMPC liposomes induced the sensorgram responses corresponding to FA-FABP3 association/dissociation kinetics. Although liposomes have been frequently utilized in SPR studies for casting lipids and membrane-associated ligands on the chip surface, to the best of our knowledge, the utilization of liposomes as carriers for highly hydrophobic analytes such as long-chained FAs has never been previously reported. FABP3 is known to receive fatty acids from neutral membranes and release them to acidic ones.[26] Thus, we chose DMPC as a carrier lipid to facilitate the binding step to the protein. Besides, DMPC forms stable liposomes under the experimental conditions. To expand the utility of this method to other fatty acids, we are seeking better carrier lipids for PUFAs and saturated FAs. Further investigations regarding applications of the current method are in progress. When non-specific interaction between the carrier lipid, DMPC, and ligands immobilized on the chip can be minimized as shown here, this strategy may serve as the last resort for estimating the affinity of lipid mediators of biomedical importance.

Acknowledgments

We are grateful to Dr. Rafael A. Espiritu for their help in the SPR experiments. We also wish to acknowledge the support given by the De La Salle University through Bro. Ricardo Laguda, FSC, Dr. Myrna Austria, Dr. Arlene Pascasio, Dr. Gerado Janairo and Dr. Marissa Noel. This work was supported in part by JSPS KAKENHI Grant Numbers 24681045, 24651244, 25242073.

Supplementary data

Supplementary data associated with this article can be found, in the online version, at http://dx.doi.org/10.1016/j.bmc.2014.02.001.

References and notes

1. Ayyer, V.; Hearty, S.; O'Kennedy, R. *Anal. Biochem.* **2010**, *407*, 165.
2. Shearer, J.; Fueger, P. T.; Rottman, J. N.; Bracy, D. P.; Binas, B.; Wasserman, D. H. *Am. J. Physiol. Endocrinol. Metab.* **2005**, *288*, E292.
3. Li, B.; Zerby, H. N.; Lee, K. *J. Anim. Sci.* **2007**, *85*, 1651.
4. Shearer, J.; Fueger, P. T.; Bracy, D. P.; Wasserman, D. H.; Rottman, J. N. *Diabetes* **2005**, *54*, 3133.
5. Shioda, N.; Yamamoto, Y.; Watanabe, M.; Binas, B.; Owada, Y.; Fukunaga, K. *J. Neurosci.* **2010**, *30*, 3146.
6. Niizeki, T.; Takeishi, Y.; Takabatake, N.; Shibata, Y.; Konta, T.; Kato, T.; Kawata, S.; Kubota, I. *Circ. J.* **2007**, *71*, 1452.
7. Kumagai, A.; Ando, R.; Miayatake, H.; Greimel, P.; Kobayashi, T.; Hirobayashi, Y.; Shimogori, T.; Miyawaki, A. *Cell* **2013**, *153*, 1602.
8. Liou, H. L.; Kahn, P.; Storch, J. *J. Biol. Chem.* **2002**, *277*, 1806.
9. Offner, G. D.; Troxler, R. F.; Brecher, P. *J. Biol. Chem.* **1986**, *261*, 5584.
10. Chmurzynska, A. *J. Appl. Genet.* **2006**, *47*, 39.
11. Corsico, B.; Cistola, D. P.; Frieden, C.; Storch, J. *Proc. Natl. Acad. Sci.* **1998**, *95*, 12174.
12. Liou, H. L.; Kahn, P. C.; Storch, J. *J. Biol. Chem.* **2002**, *277*, 1806.
13. Sacchettini, J. C.; Gordon, J. I.; Banaszak, L. J. *J. Mol. Biol.* **1989**, *208*, 327.
14. Thompson, J.; Winter, N.; Terwey, D.; Bratt, J.; Banaszak, L. *J. Biol. Chem.* **1997**, *272*, 7140.
15. Smathers, R. L.; Petersen, D. R. *Hum. Genomics* **2011**, *3*, 170.
16. Zanotti, G.; Scapin, G.; Spadon, P.; Veerkamp, J. H.; Sacchettini, J. C. *J. Biol. Chem.* **1992**, *267*, 18541.
17. Stahelin, R. V. *Mol. Biol. Cell* **2013**, *24*, 883.
18. Beniyama, Y.; Matsuno, K.; Miyachi, H. *Bioorg. Med. Chem. Lett.* **2012**, *23*, 1662.
19. Hirose, M.; Sugiyama, S.; Ishida, H.; Niiyama, M.; Matsuoka, D.; Hara, T.; Mizohata, E.; Murakami, S.; Inoue, T.; Matsuoka, S.; Murata, M. *J. Synchrotron. Radiat.* **2013**, *20*, 923.
20. Espiritu, R. A.; Matsumori, N.; Murata, M.; Nishimura, S.; Kakeya, H.; Matsunaga, S.; Yoshida, M. *Biochemistry* **2013**, *52*, 2410.
21. Sulsky, R.; Magnin, D. R.; Huang, Y.; Simpkins, L.; Taunk, P.; Patel, M.; Zhu, Y.; Stouch, T. R.; Bassolino-Klimas, D.; Parker, R.; Harrity, T.; Stoffel, R.; Taylor, D. S.; Lavoie, T. B.; Kish, K.; Jacobson, B. L.; Sheriff, S.; Adam, L. P.; Ewing, W. R.; Robl, J. A. *Bioorg. Med. Chem. Lett.* **2007**, *17*, 3511.
22. Mouri, R.; Konoki, K.; Matsumori, N.; Oishi, T.; Murata, M. *Biochemistry* **2008**, *47*, 7807.
23. Veekamp, J. H.; van Moerkerk, H. T. B.; Prinsen, C. F. M.; van Kuppevelt, T. H. *Mol. Cell. Biochem.* **1999**, *192*, 137.
24. Laughlin, R. G. In *Handbook of Detergents, Part A: Properties (Surfactant Science)*; Guy Broze, Ed., 1st ed.; CRC Press, 1999.
25. Vorum, H.; Brodersen, R.; Kragh-Hansen, U.; Pedersen, A. O. *Biochim. Biophys. Acta* **1992**, *1126*, 135.
26. Wootan, M. G.; Storch, J. *J. Biol. Chem.* **1994**, *269*, 10517.